INTERNATIONAL JOURNAL FOR NUMERICAL METHODS IN ENGINEERING
Int. J. Numer. Meth. Engng 2008; **74**:894–910
Published online 5 October 2007 in Wiley InterScience (www.interscience.wiley.com). DOI: 10.1002/nme.2193

Finite element modelling of inverse design problems in large deformations anisotropic hyperelasticity

Víctor D. Fachinotti[1,*,†], Alberto Cardona[1] and Philippe Jetteur[2]

[1]*Centro Internacional de Métodos Computacionales en Ingeniería* (*CIMEC-INTEC*), *Universidad Nacional del Litoral - CONICET*, *Güemes 3450*, *CP 3000 Santa Fe*, *Argentina*
[2]*Samtech SA*, *Parc Scientifique du Sart Tilman*, *Rue des Chasseurs-Ardennals*, *8*, *B 4031 Angleur*, *Liège*, *Belgium*

SUMMARY

This paper introduces a finite element model for the inverse design of pieces with large displacements in the elastic range. The problem consists in determining the initial shape of the piece, such that it attains the designed shape under the effect of service loads. The model is particularly focused on the design of parts with a markedly anisotropic behavior, like laminated turbine blades. Although the formulation expresses equilibrium on the distorted configuration, it uses a standard constitutive equations library that is expressed as usual for measures attached to the undistorted configuration. In this way, the modifications to a standard finite elements code are limited to the routines for the computation of the finite element internal forces and tangent matrix. Two examples are given, the first one for validation purposes, while the second is an application which has industrial interest for the design of turbine blades. Copyright © 2007 John Wiley & Sons, Ltd.

Received 11 September 2006; Revised 26 July 2007; Accepted 22 August 2007

KEY WORDS: solids; finite element method; elasticity; inverse design; anisotropic body; large deformations

1. INTRODUCTION

A central aspect when designing a piece to have an imposed shape after severe deformation is to compute its undistorted shape. In this analysis, the final (desired) configuration is supposed to be that of the piece subjected to service loads once the steady state has been attained, neglecting any transient effect.

*Correspondence to: Víctor D. Fachinotti, CIMEC-INTEC, Güemes 3450, CP 3000 Santa Fe, Argentina.
†E-mail: vfachino@intec.unl.edu.ar

Contract/grant sponsor: European Community; contract/grant number: AST4-CT-2005-516183
Contract/grant sponsor: Consejo Nacional de Investigaciones Cientìficas y Técnicas; contract/grant number: PIP 5271

The classical (direct) problem in non-linear elasticity consists in determining the distorted shape knowing the loads applied to the piece in a given reference configuration. The subject of this study is the inverse problem that consists in determining the undistorted configuration knowing the final configuration and service loads. Strictly speaking, it is an inverse 'design' problem [1], in contrast to classical inverse 'measurement' problems (often called simply 'inverse problems'), that consist in determining the material data knowing both the distorted and undistorted configurations as well as the service loads.

Some pieces (like turbine blades) that are designed to be cyclically used, must recover the original shape after each service cycle, constraining the material to lie within the elastic range all along the deformation process. Moreover, sometimes they are made of laminates with a markedly anisotropic behavior. We will use therefore an anisotropic hyperelastic material law limited to the small strains domain (however, large deformations can develop). In the isotropic case, some simplifications could be introduced that allow extending the formulation to finite hyperelasticity.

Previous numerical models for the inverse design analysis of hyperelastic bodies subjected to large deformations have been proposed by Govindjee and Mihalic [2, 3] and Yamada [4]. Both models use the finite element method in order to discretize the inverse deformation. They differ in the fact that Govindjee and Mihalic's model is Eulerian, and the equilibrium equation is formulated in terms of variables attached to the (known) distorted configuration, while Yamada's model is arbitrary Lagrangean–Eulerian, i.e. the problem is expressed on a reference configuration that is different from the undistorted and distorted ones. In Reference [3] not only the equilibrium equations but also the constitutive equations are written in terms of Eulerian variables, which complicates the description of orthotropic materials whose preferred directions are usually defined in the unknown undistorted configuration.

We made an effort in order to use the available material library from our non-linear finite element code [5], in which constitutive equations are written in terms of Lagrangean variables (Piola–Kirchhoff stresses in terms of Green–Lagrange strains). In this form, the modifications made into the code to implement the model for inverse analysis are restricted to the routines for computing the residual vector and tangent matrix for the inverse finite element method, preserving the material library, which clearly simplified the development. Another important contribution is the treatment of body forces, not included in previous works. In fact, in the problems addressed by the previous inverse design models [2–4], the body forces were not relevant. However, this is not the case when modelling turbine blades, where centrifugal body forces are significant. External forces (including body and surface forces) usually depend on deformation, with the consequent contribution to the finite element tangent matrix.

Two examples of application of the model are given. First, we consider the simple case of bending of a laminated beam, for which the determination of its distorted shape is an easy task for any available code for large deformation analysis. Once the distorted shape is known, we evaluate the ability of the present model to recover the initial shape. The second case is an industrial application for the determination of the initial shape that a laminated turbine blade should have in order to attain the desired designed shape under pressure and centrifugal loads.

2. KINEMATIC DESCRIPTION

Let $\mathscr{B}_0$ be the undistorted reference configuration of a continuum body and $\mathscr{B}$ the objective (final) configuration. The position $\mathbf{x} \in \mathscr{B}$ of any particle P with position $\mathbf{X} \in \mathscr{B}_0$ is determined by the

DOI: 10.1002/nme

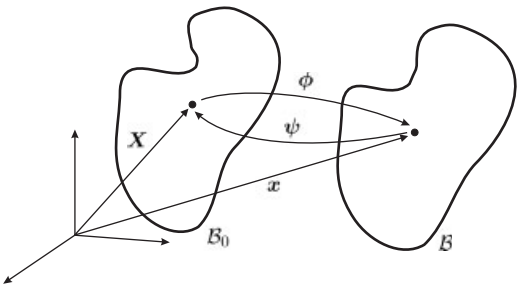

Figure 1. Distorted configuration $\mathscr{B}$, domain of inverse analysis, and undistorted configuration $\mathscr{B}_0$ sought as solution.

deformation $\mathbf{x}=\boldsymbol{\phi}(\mathbf{X})$ (Figure 1). The deformation gradient relative to the reference configuration is

$$\mathbf{F}=\mathrm{Grad}\,\boldsymbol{\phi} \tag{1}$$

where Grad denotes gradient with respect to $\mathbf{X}\in\mathscr{B}_0$.

In the problem we are interested in, we know the final configuration and we want to determine the inverse deformation $\mathbf{X}=\boldsymbol{\psi}(\mathbf{x})$ giving the position $\mathbf{X}\in\mathscr{B}_0$ of every particle whose final position is $\mathbf{x}\in\mathscr{B}$. The inverse deformation gradient is defined as

$$\mathbf{f}=\mathrm{grad}\,\boldsymbol{\psi}=\mathbf{F}^{-1} \tag{2}$$

where grad denotes gradient with respect to $\mathbf{x}\in\mathscr{B}$.

3. MATERIAL DESCRIPTION

The constitutive law for a general hyperelastic material can be written as follows [6]:

$$\mathbf{S}=\frac{\partial w}{\partial \mathbf{E}}=\mathbf{S}(\mathbf{E}) \tag{3}$$

where w is the strain-energy density function, $\mathbf{S}$ is the second Piola–Kirchhoff stress tensor, and $\mathbf{E}$ is the Green–Lagrange strain tensor defined as

$$\mathbf{E}=\tfrac{1}{2}(\mathbf{F}^{\mathrm{T}}\mathbf{F}-\mathbf{1}) \tag{4}$$

$\mathbf{1}$ denoting the second-order identity tensor.

3.1. Anisotropy in inverse analysis

The constitutive equation (3) is formulated in terms of $\mathbf{S}$ and $\mathbf{E}$, which are Lagrangean tensors, i.e. tensors related to the reference configuration. Consequently, the material properties must be attached to this configuration which is unknown. This hinders the definition of preferred material directions, and hence the modelling of anisotropic materials.

In the case of laminated bodies for which strains remain small, it is possible to approximate the preferred directions of anisotropy in the distorted configuration by writing the constitutive equation

DOI: 10.1002/nme

(3) in Eulerian form by a simple rotation of the material axes. We rotate the Green–Lagrange strain tensor and the second Piola–Kirchhoff stress tensor to the spatial axes as follows

$$\mathbf{E}^* = \mathbf{R}\mathbf{E}\mathbf{R}^{\mathrm{T}} = \tfrac{1}{2}(\mathbf{F}\mathbf{F}^{\mathrm{T}} - \mathbf{1}) = \tfrac{1}{2}(\mathbf{V}^2 - \mathbf{1}) \tag{5}$$

$$\mathbf{S}^* = \mathbf{R}\mathbf{S}\mathbf{R}^{\mathrm{T}} \tag{6}$$

where $\mathbf{V}$ is the symmetric positive-definite left-stretch tensor and $\mathbf{R}$ is the rotation tensor, both being computed from the polar decomposition of the deformation gradient:

$$\mathbf{F} = \mathbf{V}\mathbf{R} \tag{7}$$

Now, the chain rule together with Equation (5) yields

$$S_{ij} = \frac{\partial w}{\partial E_{ij}} = \frac{\partial w}{\partial E^*_{kl}} \frac{\partial E^*_{kl}}{\partial E_{ij}} = R_{ki} R_{lj} \frac{\partial w}{\partial E^*_{kl}} \quad \text{or} \quad \mathbf{S} = \mathbf{R}^{\mathrm{T}} \frac{\partial w}{\partial \mathbf{E}^*} \mathbf{R} \tag{8}$$

from which we deduce the desired constitutive law in the Eulerian form as

$$\mathbf{S}^* = \frac{\partial w}{\partial \mathbf{E}^*} = \mathbf{S}^*(\mathbf{E}^*) \tag{9}$$

In such a way, we are able to define the material properties with respect to a system of axes linked to the known distorted configuration.

4. FINITE ELEMENT FORMULATION

The inverse design problem consists in finding the function $\boldsymbol{\psi}$ that satisfies the equilibrium equations, taken here in the weak form as

$$\int_{\mathscr{B}} \mathrm{tr}[\boldsymbol{\sigma}^{\mathrm{T}} \mathrm{grad}(\boldsymbol{\eta})] \mathrm{d}v - \int_{\mathscr{B}} \mathbf{b} \cdot \boldsymbol{\eta} \, \mathrm{d}v - \int_{\partial \mathscr{B}_t} \mathbf{t} \cdot \boldsymbol{\eta} \, \mathrm{d}s = \mathbf{0} \tag{10}$$

for every admissible variation $\boldsymbol{\eta}$, where $\boldsymbol{\sigma}$ is the Cauchy stress tensor, $\mathbf{b}$ is the given body force per unit distorted volume and $\mathbf{t}$ is the traction prescribed on the portion $\partial \mathscr{B}_t$ of the boundary $\partial \mathscr{B}$ of the distorted domain $\mathscr{B}$ (hence, $\mathbf{t}$ is a force per unit distorted area).

Using the finite element method, the position of particles in the undistorted configuration is approximated inside a typical finite element Ω^e with nodes $1, 2, \ldots, N$ as follows:

$$\mathbf{X} \approx \sum_{I=1}^{N} N_I(\mathbf{x}) \mathbf{X}_I \tag{11}$$

where $N_I(\mathbf{x})$ is the shape function associated with the node I, and $\mathbf{X}_I$ is the unknown position of this node in the undistorted configuration.

Introducing this approximation, and taking variations with respect to the positions in the undistorted configuration (standard Galerkin formulation), we obtain the discrete equation

$$\mathbf{R} = \mathbf{F}^{\mathrm{int}} - \mathbf{F}^{\mathrm{ext}} = \mathbf{0} \tag{12}$$

DOI: 10.1002/nme

where $\mathbf{F}^{\text{int}}$ and $\mathbf{F}^{\text{ext}}$ are, respectively, the internal and external force vectors, given by

$$\mathbf{F}^{\text{int}} = \int_{\mathscr{B}} \mathbf{B}^{\mathrm{T}} \bar{\boldsymbol{\sigma}} \, \mathrm{d}v \tag{13}$$

$$\mathbf{F}^{\text{ext}} = \int_{\mathscr{B}} \mathbf{N}^{\mathrm{T}} \mathbf{b} \, \mathrm{d}v + \int_{\partial \mathscr{B}_t} \mathbf{N}^{\mathrm{T}} \mathbf{t} \, \mathrm{d}s \tag{14}$$

where $\mathbf{B}$ is the gradients matrix, and $\bar{\boldsymbol{\sigma}}$ the vector containing the independent components of the symmetric Cauchy stress tensor $\boldsymbol{\sigma}$.[‡]

In turbine blades modelling, the external forces mainly consist of the centrifugal and pressure forces. The former are represented by the first term of the r.h.s. of Equation (14) with $\mathbf{b}$ defined as

$$\mathbf{b} = \rho \mathbf{a}^{\text{centr}} \tag{15}$$

being ρ the density in the distorted configuration, and $\mathbf{a}^{\text{centr}}$ the centrifugal acceleration, defined as

$$\mathbf{a}^{\text{centr}}(\mathbf{x}) = \boldsymbol{\omega} \times [\boldsymbol{\omega} \times (\mathbf{x} - \mathbf{o})] \tag{16}$$

where $\boldsymbol{\omega}$ is the angular velocity vector and $\mathbf{o}$ the position of an arbitrary point on the rotation axis. On the other hand, the pressure force is represented by the second term of the r.h.s. of Equation (14) by defining

$$\mathbf{t} = -p\mathbf{n} \tag{17}$$

where p is the pressure and $\mathbf{n}$ the outer normal to the portion $\partial \mathscr{B}_t$ of the surface of the body in the distorted configuration.

4.1. Computation of strains and stresses in finite elements

Using Equation (11), the inverse deformation gradient is approximated in terms of derivatives of the interpolation functions as

$$\mathbf{f} = \frac{\partial \mathbf{X}}{\partial \mathbf{x}} \approx \frac{\partial N_I}{\partial \mathbf{x}} \mathbf{X}_I \tag{18}$$

Once $\mathbf{f}$ is known, we can compute the (direct) deformation gradient $\mathbf{F} = \mathbf{f}^{-1}$, and then the Green–Lagrange strain $\mathbf{E}$ using Equation (4) as well as its rotated counterpart $\mathbf{E}^*$ given by Equation (5).

Entering $\mathbf{E}^*$ in the constitutive law (9), we determine the rotated second Piola–Kirchhoff stress $\mathbf{S}^*$. Then, we are able to compute the Cauchy stress by means of the relationship

$$\boldsymbol{\sigma} = j\mathbf{F}\mathbf{S}\mathbf{F}^{\mathrm{T}} = j\mathbf{V}\mathbf{S}^*\mathbf{V}^{\mathrm{T}}$$

or, given in Cartesian components as

$$\sigma_{kl} = j V_{km} S^*_{mn} V_{ln} \tag{19}$$

[‡]From now on, $\bar{\mathbf{T}}$ denotes the vector (matrix) containing the components of the second-order (respectively, fourth-order) tensor $\mathbf{T}$. A single rule for the mapping of tensors into vectors or matrices cannot be defined, since the mapping depends on the tensor symmetries involved in certain tensor products. For the sake of conciseness, the definition of the algorithmic versions of all tensors appearing in the text is given in the Appendix.

DOI: 10.1002/nme

where $j = \det \mathbf{f}$ is the Jacobian of the inverse deformation $\mathbf{X} = \boldsymbol{\psi}(\mathbf{x})$. In order to replace tensor products by matrix products as usual in the finite element practice, we introduce the tensor

$$I^V_{klmn} = \tfrac{1}{2}(V_{km}V_{ln} + V_{kn}V_{lm}) = I^V_{klnm} = I^V_{lkmn} \tag{20}$$

which allows us to rewrite (19) as follows:

$$\sigma_{kl} = j\, I^V_{klmn} S^*_{mn} \tag{21}$$

A tensor product like this can be taken to the following matrix expression:

$$\bar{\boldsymbol{\sigma}} = j\bar{\mathbf{I}}^V \bar{\mathbf{S}}^* \tag{22}$$

4.2. Solution of the non-linear equilibrium equation

The non-linear equation (12) is solved iteratively using the Newton–Raphson method (see [7] for details on the implementation of this method in the finite element context). At each iteration k we have to solve the following linear equation for the increment $\Delta\mathbf{q}$:

$$\mathbf{R}(\mathbf{q}^{k+1}) = \mathbf{R}(\mathbf{q}^k) + \mathbf{K}(\mathbf{q}^k)\Delta\mathbf{q} \tag{23}$$

where $\mathbf{K}$ denotes the tangent matrix, given by

$$\mathbf{K} = \frac{\partial \mathbf{R}}{\partial \mathbf{q}} = \frac{\partial \mathbf{F}^{\text{int}}}{\partial \mathbf{q}} + \frac{\partial \mathbf{F}^{\text{ext}}}{\partial \mathbf{q}} = \mathbf{K}^{\text{int}} + \mathbf{K}^{\text{ext}} \tag{24}$$

and where $\mathbf{q}$ is the vector of unknown nodal parameters, which in this case are the positions $\mathbf{X}_I$ of nodes at the initial configuration.

Concerning external forces, we note that there is no contribution to the tangent matrix from the pressure forces in inverse analysis. In fact, contrary to what happens in direct analysis, the normal $\mathbf{n}$ to the external surface in the distorted configuration is known and fixed. On the other hand, there would be no contribution from the centrifugal force vector if ρ were known in the distorted configuration. However, the value of the density we usually know is that related to the undistorted configuration, say ρ_0. Then, ρ is computed from the local mass balance equation

$$\rho = j\rho_0 \tag{25}$$

Nevertheless, since we remain within the domain of small strains, the density $\rho \approx \rho_0$ and the contribution of the centrifugal forces to the tangent matrix can be neglected.

Therefore, the tangent matrix reduces to the expression

$$\mathbf{K} \approx \mathbf{K}^{\text{int}} = \int_{\mathscr{B}} \mathbf{B}^{\mathrm{T}} \frac{\partial \bar{\boldsymbol{\sigma}}}{\partial \mathbf{q}}\, \mathrm{d}v \tag{26}$$

The computation of $\partial\bar{\boldsymbol{\sigma}}/\partial\mathbf{q}$ in an exact analytical way is described in the next section.

4.3. Computation of the stress derivatives

In a typical finite element, after computing the internal forces vector as described above, we know the inverse deformation gradient $\mathbf{f}$, the deformation gradient $\mathbf{F}$, the left-stretch tensor $\mathbf{V}$, and the fourth-order tensor $\mathbf{I}^V$ (which is a function of $\mathbf{V}$ squared), the rotated Green–Lagrange strain $\mathbf{E}^*$,

DOI: 10.1002/nme

the rotated Piola–Kirchhoff stress $\mathbf{S}^*$, and the Cauchy stress $\boldsymbol{\sigma}$. In order to compute the tangent stiffness matrix for inverse analysis, we need to compute the derivatives of the Cauchy stress with respect to nodal parameters of the inverse motion. For this purpose, we will compute first the corresponding variations:

$$\Delta\bar{\boldsymbol{\sigma}} = \underbrace{j^{-1}\bar{\boldsymbol{\sigma}}\Delta j}_{\bar{\boldsymbol{\Delta}}^{(1)}} + \underbrace{j\bar{\mathbf{I}}^V\Delta\bar{\mathbf{S}}^*}_{\bar{\boldsymbol{\Delta}}^{(2)}} + \underbrace{j\Delta\bar{\mathbf{I}}^V\bar{\mathbf{S}}^*}_{\bar{\boldsymbol{\Delta}}^{(3)}} \tag{27}$$

For clarity of presentation, the computation of each term $\bar{\boldsymbol{\Delta}}^{(i)}$ will be treated separately.

4.3.1. Computation of $\bar{\boldsymbol{\Delta}}^{(1)}$. The differentiation rule for the determinant of a second-order tensor yields

$$\Delta j = j\,\mathrm{tr}(\mathbf{F}^{\mathrm{T}}\Delta\mathbf{f}) = j\,(\bar{\mathbf{F}}^{\mathrm{T}})^{\mathrm{T}}\Delta\bar{\mathbf{f}} \tag{28}$$

Given $\mathbf{f}$ by Equation (18), it is straightforward to compute its determinant j, its inverse $\mathbf{F}$ and its derivative

$$\Delta\mathbf{f} = \frac{\partial N_I}{\partial\mathbf{x}}\Delta\mathbf{X}x_I \quad \text{or} \quad \Delta\bar{\mathbf{f}} = \bar{\mathbf{N}}_{,x}\Delta\mathbf{q} \tag{29}$$

Then, the first term in the r.h.s. of Equation (27) can be expressed as

$$\bar{\boldsymbol{\Delta}}^{(1)} = \bar{\boldsymbol{\sigma}}(\bar{\mathbf{F}}^{\mathrm{T}})^{\mathrm{T}}\bar{\mathbf{N}}_{,x}\Delta\mathbf{q} \tag{30}$$

4.3.2. Computation of $\bar{\boldsymbol{\Delta}}^{(2)}$. First, we need to determine

$$\Delta\mathbf{S}^* = \frac{\partial\mathbf{S}^*}{\partial\mathbf{E}^*}\Delta\mathbf{E}^* = \mathbf{D}^*\Delta\mathbf{E}^* \tag{31}$$

The components D^*_{mnkl} of the fourth-order tensor $\mathbf{D}^*$ of tangent moduli, together with the rotated second Piola–Kirchhoff stress tensor $\mathbf{S}^*$, are computed in the constitutive equation software module as a function of the rotated Green–Lagrange strain $\mathbf{E}^*$. The tensor $\mathbf{D}^*$ verifies the following symmetries:

$$D^*_{mnkl} = D^*_{nmkl} = D^*_{mnlk} \tag{32}$$

On the other hand, the variation of $\mathbf{E}^*$ results

$$\Delta E^*_{ij} = \tfrac{1}{2}\Delta(F_{ik}F_{jk}) = \Theta_{ijkl}\Delta F_{kl} \quad \text{or} \quad \Delta\bar{\mathbf{E}}^* = \bar{\boldsymbol{\Theta}}\Delta\bar{\mathbf{F}} \tag{33}$$

with the components of the fourth-order tensor $\boldsymbol{\Theta}$ given by

$$\Theta_{ijkl} = \tfrac{1}{2}(\delta_{ik}F_{jl} + \delta_{jk}F_{il}) \tag{34}$$

where δ_{ij} denotes the Kronecker delta.

Using the rule of differentiation of the inverse of a second-order tensor, we obtain

$$\Delta F_{km} = -\Lambda_{kmpq}\Delta f_{pq} \quad \text{or} \quad \Delta\bar{\mathbf{F}} = -\bar{\boldsymbol{\Lambda}}\Delta\bar{\mathbf{f}} \tag{35}$$

DOI: 10.1002/nme

with

$$\Lambda_{kmpq} = F_{kp} F_{qm} \tag{36}$$

Then, the second term in the r.h.s. of Equation (27) can be expressed as

$$\bar{\boldsymbol{\Delta}}^{(2)} = -j\bar{\mathbf{I}}^{V}\bar{\mathbf{D}}^{*}\bar{\boldsymbol{\Theta}}\bar{\boldsymbol{\Lambda}}\bar{\mathbf{N}}_{,x}\Delta\mathbf{q} \tag{37}$$

4.3.3. Computation of $\bar{\boldsymbol{\Delta}}^{(3)}$. First, let us rewrite the third term of the r.h.s. of Equation (27) as follows:

$$\Delta^{(3)}_{kl} = j\Delta I^{V}_{klmn} S^{*}_{mn} = j\Upsilon_{klpq}\Delta V_{pq} \quad \text{or} \quad \bar{\boldsymbol{\Delta}}^{(3)} = j\,\bar{\boldsymbol{\Upsilon}}\Delta\bar{\mathbf{V}} \tag{38}$$

where

$$\Upsilon_{klpq} = \left(I_{kmpq}V_{ln} + I_{lmpq}V_{kn}\right) S^{*}_{mn} = \Upsilon_{lkpq} = \Upsilon_{klqp} \tag{39}$$

Here, $I_{ijkl} = (\delta_{ik}\delta_{jl} + \delta_{il}\delta_{jl})/2$ is the fourth-order identity tensor.

Now, the only missing term to be computed is $\Delta\mathbf{V}$. To this end, we begin by computing $\Delta\mathbf{V}^2$:

$$\Delta(V_{ik}V_{kj}) = \Delta V_{ik}V_{kj} + V_{ik}\Delta V_{kj} = \Phi_{ijkm}\Delta V_{km} \quad \text{or} \quad \Delta\bar{\mathbf{V}}^2 = \bar{\boldsymbol{\Phi}}\Delta\bar{\mathbf{V}} \tag{40}$$

where

$$\Phi_{ijkm} = I_{ijkl}V_{lm} + I_{ijml}V_{lk} = \Phi_{ijmk} = \Phi_{jikm} \tag{41}$$

On the other hand, since $\mathbf{V}^2 = 2\mathbf{E}^{*} - \mathbf{1}$, its variation can also be computed as

$$\Delta\bar{\mathbf{V}}^2 = 2\Delta\bar{\mathbf{E}}^{*} = -2\bar{\boldsymbol{\Theta}}\bar{\boldsymbol{\Lambda}}\bar{\mathbf{N}}_{,x}\Delta\mathbf{q} \tag{42}$$

By making Equation (40) the same as Equation (42), we obtain

$$\Delta\bar{\mathbf{V}} = -2\bar{\boldsymbol{\Phi}}^{-1}\bar{\boldsymbol{\Theta}}\bar{\boldsymbol{\Lambda}}\bar{\mathbf{N}}_{,x}\Delta\mathbf{q} \tag{43}$$

Finally, after replacing the last equation into Equation (38), the third term of the r.h.s. of Equation (27) can be expressed as

$$\bar{\boldsymbol{\Delta}}^{(3)} = -2j\bar{\boldsymbol{\Upsilon}}\bar{\boldsymbol{\Phi}}^{-1}\bar{\boldsymbol{\Theta}}\bar{\boldsymbol{\Lambda}}\bar{\mathbf{N}}_{,x}\Delta\mathbf{q} \tag{44}$$

4.3.4. Final form of $\partial\bar{\boldsymbol{\sigma}}/\partial\mathbf{q}$. The form given to the terms $\bar{\boldsymbol{\Delta}}^{(i)}$ of the variation of $\bar{\boldsymbol{\sigma}}$ allows the immediate determination of the derivative of $\bar{\boldsymbol{\sigma}}$ with respect to the nodal unknowns $\mathbf{q}$:

$$\frac{\partial\bar{\boldsymbol{\sigma}}}{\partial\mathbf{q}} = \bar{\boldsymbol{\sigma}}(\bar{\mathbf{F}}^{\mathrm{T}})^{\mathrm{T}}\bar{\mathbf{N}}_{,x} - j\bar{\mathbf{I}}^{V}\bar{\mathbf{D}}^{*}\bar{\boldsymbol{\Theta}}\bar{\boldsymbol{\Lambda}}\bar{\mathbf{N}}_{,x} - 2j\bar{\boldsymbol{\Upsilon}}\bar{\boldsymbol{\Phi}}^{-1}\bar{\boldsymbol{\Theta}}\bar{\boldsymbol{\Lambda}}\bar{\mathbf{N}}_{,x} \tag{45}$$

Therefore, the tangent stiffness matrix results

$$\mathbf{K} = \int_{\mathscr{B}} \mathbf{B}^{\mathrm{T}}[\bar{\boldsymbol{\sigma}}(\bar{\mathbf{F}}^{\mathrm{T}})^{\mathrm{T}} - j\bar{\mathbf{I}}^{V}\bar{\mathbf{D}}^{*}\bar{\boldsymbol{\Theta}}\bar{\boldsymbol{\Lambda}} - 2j\bar{\boldsymbol{\Upsilon}}\bar{\boldsymbol{\Phi}}^{-1}\bar{\boldsymbol{\Theta}}\bar{\boldsymbol{\Lambda}}]\bar{\mathbf{N}}_{,x}\,\mathrm{d}v \tag{46}$$

Note that $\mathbf{K}$ is non-symmetric, as it was already the case in References [2, 3].

Although not detailed here, the formulation can be easily extended to account also for thermal loads.

DOI: 10.1002/nme

Remark
In this work, the use of a constitutive law of the type $\mathbf{S}^* = \mathbf{S}^*(\mathbf{E}^*)$ makes the linearization of stress with respect to material coordinates somehow different to what can be found in preceding works on inverse analysis, where different constitutive laws were used.

For instance, in the work of Govindjee and Mihalic [2] they used a neo-Hookean isotropic material model defined by

$$\sigma_{kl} = j\,\mu(c_{kl}^{-1} - \delta_{kl}) - \lambda j \ln j\,\delta_{kl} \tag{47}$$

where $\mathbf{c} = \mathbf{f}^{\mathrm{T}}\mathbf{f}$, and λ and μ are material parameters that reduce to the Lamé constants in the case of small strains. Then, they obtain

$$D^{\sigma}_{klmn} = \frac{\partial \sigma_{kl}}{\partial c_{mn}} = \tfrac{1}{2} j\{\mu(c_{kl}^{-1}c_{mn}^{-1} - c_{km}^{-1}c_{ln}^{-1} - c_{kn}^{-1}c_{lm}^{-1}) - [\mu + \lambda(1 - \ln j)]\delta_{kl}c_{mn}^{-1}\} \tag{48}$$

The variation of $\boldsymbol{\sigma}$ is completely determined after computing

$$\Delta c_{mn} = 2\theta_{mnkl}\Delta f_{kl} \quad \text{or} \quad \Delta\bar{\mathbf{c}} = 2\bar{\boldsymbol{\theta}}\Delta\bar{\mathbf{f}} \tag{49}$$

with

$$\theta_{mnkl} = \tfrac{1}{2}(\delta_{ml} f_{kn} + \delta_{nl} f_{km}) \tag{50}$$

Therefore, using a constitutive equation of the type $\boldsymbol{\sigma} = \boldsymbol{\sigma}(\mathbf{c})$ similar to Equation (47), the derivative of $\boldsymbol{\sigma}$ with respect to the material coordinates takes the algorithmic form

$$\frac{\partial \bar{\boldsymbol{\sigma}}}{\partial \mathbf{q}} = 2\bar{\mathbf{D}}^{\sigma}\bar{\boldsymbol{\theta}}\bar{\mathbf{N}}_{,x} \tag{51}$$

which is much simpler than that of Equation (45) used in this work. Unfortunately, we cannot define a law $\boldsymbol{\sigma} = \boldsymbol{\sigma}(\mathbf{c})$ in the case of anisotropic behavior [8].

Note finally that linearization of stresses with respect to material coordinates has been used in other contexts by several authors, for instance, in the work of Thoutireddy and Ortiz [9, 10] on shape optimization and mesh adaptivity. They use constitutive laws of the form

$$\mathbf{P} = \frac{\partial w}{\partial \mathbf{F}} \tag{52}$$

where $\mathbf{P}$ is the first Piola–Kirchhoff stress tensor, from which they derive the moduli $D^{P}_{ijkl} = \partial P_{ij}/\partial F_{kl}$. Then, the variation of $\boldsymbol{\sigma} = j\mathbf{P}\mathbf{F}^{\mathrm{T}}$ takes the form

$$\Delta\sigma_{kl} = \frac{1}{j}\sigma_{kl}\Delta j + j\,D^{P}_{kmpq}\Delta F_{pq}\,F_{lm} + j\,P_{km}\Delta F_{lm} \tag{53}$$

This linearization is also somehow simpler than the linearization defined by Equation (45). Let us remark that law (52) may be used for anisotropic materials and is not restricted to isotropy, hence it could have been used in the present formulation for inverse design problems, after applying a similar technique of rotation of axes to be able to define material properties in a system of axes linked to the distorted (known) configuration. Nevertheless, in our case a law of the type $\mathbf{S}^* = \mathbf{S}^*(\mathbf{E}^*)$ was necessary with the objective of reutilization of the available material software module.

DOI: 10.1002/nme

5. APPLICATION

5.1. Validation test

Let us consider the simple problem of bending a beam under plane strain conditions. First, we solve the direct problem, i.e. given the undistorted configuration $\mathscr{B}_0$ as well as the kinematic boundary conditions and the applied forces, we determine the distorted configuration $\mathscr{B}$. The problem is schematized in Figure 2. The domain is discretized using trilinear hexahedral finite elements. Even if it is essentially a 2D problem, 3D elements are used for generality. In order to represent a plane strain state, a one-element-wide mesh is used, and the faces normal to the **k**-axis are constrained to move in their planes.

The bar is made of horizontal laminates with fibers disposed in the **i**-direction. The material has an orthotropic behavior, characterized by Young's moduli E_1, E_2, E_3, the Poisson ratii $\nu_{12}, \nu_{23}, \nu_{13}$, and shear ratii G_{12}, G_{23}, G_{13} with respect to the orthotropy orthogonal axes $\{\mathbf{u}^{(1)}, \mathbf{u}^{(2)}, \mathbf{u}^{(3)}\}$. Table I lists the values we assumed for these properties. Further, we adopt the hyperelastic constitutive law as

$$\bar{\mathbf{S}} = \bar{\mathbf{D}}\bar{\mathbf{E}} \tag{54}$$

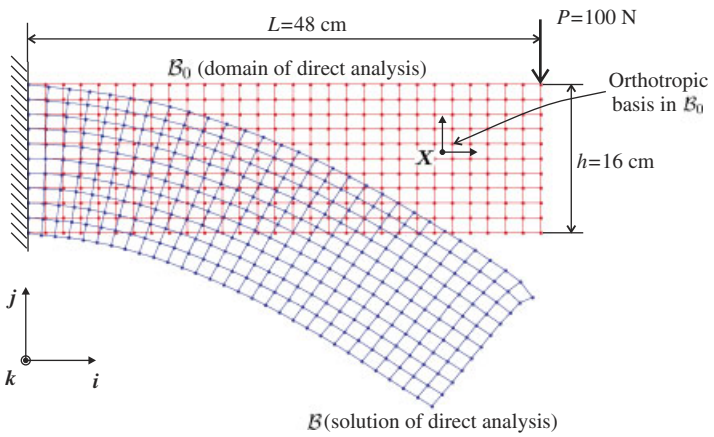

Figure 2. Direct problem.

Table I. Material data for the beam bending problem.

$E_1 = 500$ N/cm^2	$\nu_{12} = 0.3$	$G_{12} = 192.31$ N/cm^2
$E_2 = 1000$ N/cm^2	$\nu_{23} = 0.2$	$G_{23} = 312.50$ N/cm^2
$E_3 = 750$ N/cm^2	$\nu_{13} = 0.25$	$G_{13} = 288.46$ N/cm^2

DOI: 10.1002/nme

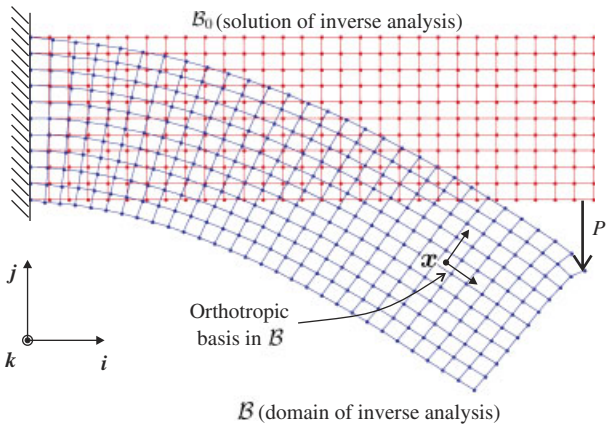

Figure 3. Inverse problem.

where

$$\bar{\mathbf{D}} = \begin{bmatrix} \frac{1-\nu_{23}\nu_{32}}{\alpha E_2 E_3} & \frac{\nu_{12}+\nu_{32}\nu_{13}}{\alpha E_1 E_3} & \frac{\nu_{13}+\nu_{12}\nu_{23}}{\alpha E_1 E_2} & 0 & 0 & 0 \\ & \frac{1-\nu_{13}\nu_{31}}{\alpha E_3 E_3} & \frac{\nu_{23}+\nu_{21}\nu_{13}}{\alpha E_1 E_2} & 0 & 0 & 0 \\ & & \frac{1-\nu_{12}\nu_{21}}{\alpha E_1 E_2} & 0 & 0 & 0 \\ & & & G_{12} & 0 & 0 \\ & \text{symmetric} & & & G_{23} & 0 \\ & & & & & G_{13} \end{bmatrix} \tag{55}$$

with

$$\begin{gathered} \nu_{21} = \frac{E_2}{E_1}\nu_{12}, \quad \nu_{31} = \frac{E_3}{E_1}\nu_{13}, \quad \nu_{32} = \frac{E_3}{E_2}\nu_{23} \\ \alpha = \frac{1-\nu_{12}\nu_{21}-\nu_{23}\nu_{32}-\nu_{13}\nu_{31}-2\nu_{12}\nu_{32}\nu_{13}}{E_1 E_2 E_3} \end{gathered} \tag{56}$$

Here, the orthotropy axes $\{\mathbf{u}^{(1)}, \mathbf{u}^{(2)}, \mathbf{u}^{(3)}\}$ coincide with the Lagrangean principal axes, which are also coincident with the Cartesian coordinate basis $\{\mathbf{i}, \mathbf{j}, \mathbf{k}\}$.

The domain of the inverse design analysis is the distorted configuration $\mathcal{B}$ computed as solution of the direct analysis and shown in Figure 2. The inverse problem is schematized in Figure 3. The objective of the computation is to verify if we are able to recover the original undistorted configuration as solution.

DOI: 10.1002/nme

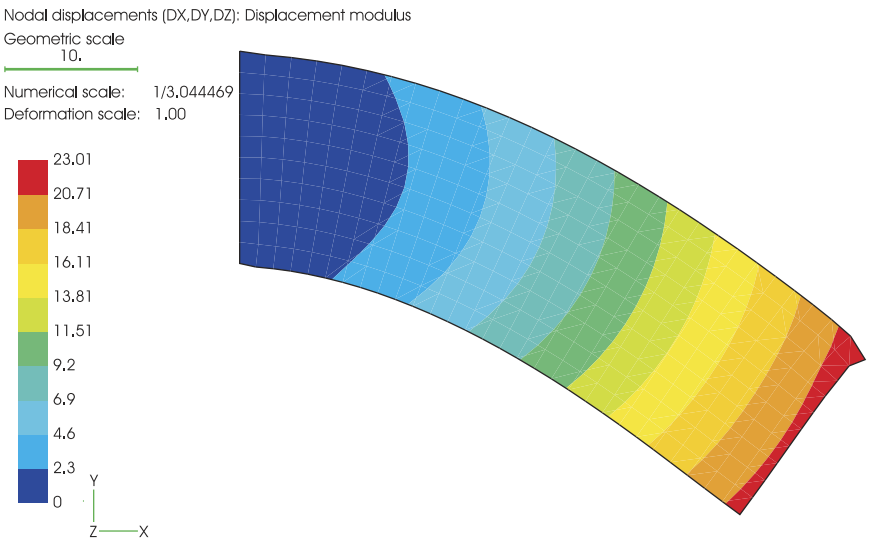

Figure 4. Displacement modulus from the inverse analysis.

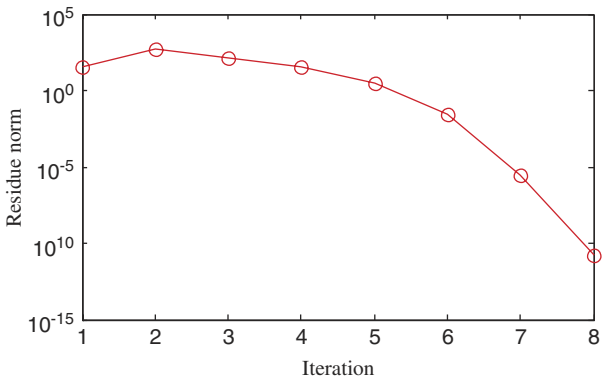

Figure 5. Evolution of the residue norm during the inverse analysis.

The orthotropy axes coincide now with the Eulerian principal axes $\mathbf{v}^{(i)} = \mathbf{R}\mathbf{u}^{(i)}$, where $\mathbf{R}$ is the rotational part of the deformation gradient $\mathbf{F}$ and varies throughout the domain. Although in this case these axes can be exactly determined from the previous direct analysis, in practice they will be given for the distorted geometry taking into account the laminated nature of the body and the desired fiber orientations when under loading.

Figure 4 shows a plot of the inverse solution, displaying a map of the magnitude of the displacements $\mathbf{u} = \mathbf{x} - \boldsymbol{\psi}(\mathbf{x})$.

We define an error measure of the inverse model computation, as a distance between the nodes of the mesh used for the direct analysis and the positions obtained as solution of the

DOI: 10.1002/nme

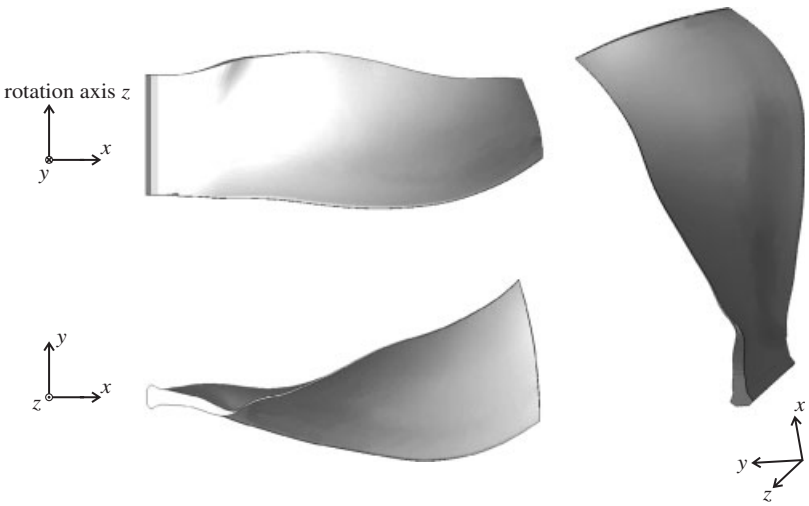

Figure 6. Inverse analysis of the turbine blade. Distorted shape from different points of view.

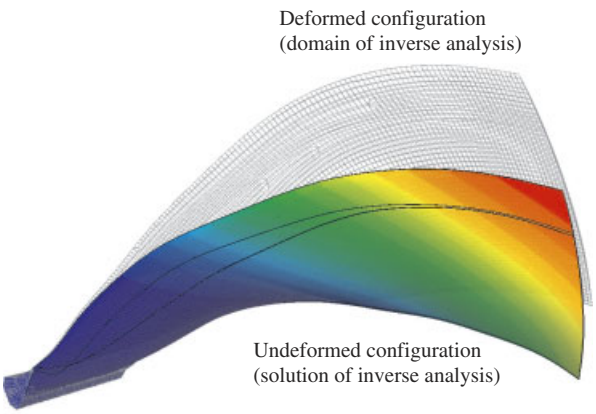

Figure 7. Inverse analysis of the turbine blade. Distorted *versus* undistorted shapes and displacement modulus.

inverse analysis. After solving the equilibrium equation (12) with a very small residue norm $\|\mathbf{R}\| < 1.6 \times 10^{-11}$ (the L_2-norm of the residue vector $\mathbf{R}$), we obtained a maximum error of 26.6 μm at the nodes where the concentrated forces were applied. The relative error with respect to the displacements magnitude is less than 0.01%, which demonstrates the excellent accuracy of the inverse model.

Figure 5 shows the evolution of $\|\mathbf{R}\|$ as a function of iterations. We note that after the fifth iteration, when the trial solution entered into the convergence radius of the solution, an optimal (quadratic) convergence rate is observed.

DOI: 10.1002/nme

5.2. *Industrial application*

The inverse model is applied now to a real case: the design of a laminated turbine blade, subjected to pressure and centrifugal forces. The blade has a complex shape determined by the fluid mechanics design for the loaded configuration. The objective of the computation is to determine the initial unloaded shape so that the blade shape in operation matches that imposed by the fluid mechanics design.

The material behavior is described using an hyperelastic constitutive law. The blade in distorted configuration is discretized using trilinear hexahedral finite elements. Figure 6 displays three views of the distorted blade geometry.

In Figure 7, the undistorted shape obtained from the inverse analysis is superposed to the distorted mesh. Let us note that geometrical and deformation scales are coincident in Figure 7, so that the deformations involved in the problem are large well entering into the geometric non-linear regime.

In order to solve the non-linear equation (12), it was necessary to increase gradually the loading in some steps (the final step corresponding to the whole pressure and centrifugal loading applied to the blade), the solution of each step taken as initial guess for the following step. The inverse analysis has converged with an average of 3.5 iterations per step.

6. CONCLUSIONS

The present work introduced a finite element model for the inverse design analysis of 3D geometrically non-linear statics problems with hyperelastic materials.

Anisotropic materials were handled without modifying the constitutive equation software module developed for classical (direct) large deformation elastic analysis. An exact computation of the tangent matrix made possible to obtain an optimum convergence rate.

An example showed the excellent accuracy of the model, measured by its ability to recover the original mesh of the corresponding direct analysis. Also, an example of application to the computation of the initial shape of a turbine blade subjected to pressure and centrifugal loads has been shown.

APPENDIX: ALGORITHMIC FORM OF TENSORS

A symmetric stress tensor, e.g. $\boldsymbol{\sigma}$, is mapped in a vector according to the rule

$$\bar{\boldsymbol{\sigma}} = \bar{\mathbf{v}}^{\sigma}(\boldsymbol{\sigma}) = [\sigma_{11} \;\; \sigma_{22} \;\; \sigma_{33} \;\; \sigma_{12} \;\; \sigma_{23} \;\; \sigma_{31}]^{\mathrm{T}}$$

Accordingly, $\bar{\mathbf{S}} = \bar{\mathbf{v}}^{\sigma}(\mathbf{S})$, $\bar{\mathbf{S}}^{*} = \bar{\mathbf{v}}^{\sigma}(\mathbf{S}^{*})$, $\bar{\Delta}^{(i)} = \bar{\mathbf{v}}^{\sigma}(\Delta^{(i)})$.

For a symmetric strain tensor, say $\mathbf{E}$, the following rule holds:

$$\bar{\mathbf{E}} = \bar{\mathbf{v}}^{\varepsilon}(\mathbf{E}) = [E_{11} \;\; E_{22} \;\; E_{33} \;\; 2E_{12} \;\; 2E_{23} \;\; 2E_{31}]^{\mathrm{T}}$$

and so as $\bar{\mathbf{E}}^{*} = \bar{\mathbf{v}}^{\varepsilon}(\mathbf{E}^{*})$, $\bar{\mathbf{c}} = \bar{\mathbf{v}}^{\varepsilon}(\mathbf{c})$ and $\bar{\mathbf{V}}^{2} = \bar{\mathbf{v}}^{\varepsilon}(\mathbf{V}^{2})$. This convention is adopted also for the left-stretch tensor $\mathbf{V}$, which transforms to $\bar{\mathbf{V}} = \bar{\mathbf{v}}^{\varepsilon}(\mathbf{V})$.

DOI: 10.1002/nme

For non-symmetric second-order tensors like $\mathbf{f}$, having nine independent components, we apply the transformation:

$$\bar{\mathbf{f}} = \bar{\mathbf{v}}^f(\mathbf{f}) = [f_{11} \;\; f_{21} \;\; f_{31} \;\; f_{12} \;\; f_{22} \;\; f_{32} \;\; f_{13} \;\; f_{23} \;\; f_{33}]^{\mathrm{T}}$$

hence, $\bar{\mathbf{F}}^{\mathrm{T}} = \mathbf{v}^f(\mathbf{F}^{\mathrm{T}})$, $\mathbf{E}^*$, and $\mathbf{c}$. This is also the case for the symmetric strain-like tensor $\mathbf{c}$.

Fourth-order tensors $\mathbf{T}$ having the symmetries $T_{ijkl} = T_{jikl} = T_{ijlk}$ are mapped into matrices whose general expression is

$$\bar{\mathbf{T}} = \bar{\mathbf{M}}^s(\mathbf{T}, \alpha, \beta) = \begin{bmatrix} T_{1111} & T_{1122} & T_{1133} & \alpha T_{1112} & \alpha T_{1123} & \alpha T_{1131} \\ T_{2211} & T_{2222} & T_{2233} & \alpha T_{2212} & \alpha T_{2223} & \alpha T_{2231} \\ T_{3311} & T_{3322} & T_{3333} & \alpha T_{3312} & \alpha T_{3323} & \alpha T_{3331} \\ \beta T_{1211} & \beta T_{1222} & \beta T_{1233} & \alpha\beta T_{1212} & \alpha\beta T_{1223} & \alpha\beta T_{1231} \\ \beta T_{2311} & \beta T_{2322} & \beta T_{2333} & \alpha\beta T_{2312} & \alpha\beta T_{2323} & \alpha\beta T_{2331} \\ \beta T_{3111} & \beta T_{3122} & \beta T_{3133} & \alpha\beta T_{3112} & \alpha\beta T_{3123} & \alpha\beta T_{3131} \end{bmatrix} \tag{A1}$$

where the coefficients α and β depend on the nature of the second-order tensors involved in the tensor product we aim to replace by a simpler matrix product. For tensors like $\mathbf{D}$, $\mathbf{D}^*$, $\mathbf{D}^\sigma$, and $\boldsymbol{\Upsilon}$ that are multiplied by a symmetric strain tensor to obtain a symmetric stress tensor, we have $\alpha = \beta = 1$. On the other hand, the tensor $\mathbf{I}^V$ relating two symmetric stress tensors in Equation (38) is mapped into the matrix $\bar{\mathbf{I}}^V = \bar{\mathbf{M}}^s(\mathbf{I}^V, 2, 1)$. It is the same case for $\boldsymbol{\Phi}$ relating $\Delta\mathbf{V}^2$ and $\Delta\mathbf{V}$ in Equation (40), which maps into $\bar{\boldsymbol{\Phi}} = \bar{\mathbf{M}}^s(\boldsymbol{\Phi}, 2, 1)$.

Special mappings are needed for fourth-order tensors without such symmetries. For tensor $\boldsymbol{\Theta}$ relating the symmetric strain tensor $\Delta\mathbf{E}^*$ and the non-symmetric tensor $\Delta\mathbf{F}$ in Equation (33), we have

$$\bar{\boldsymbol{\Theta}} = \begin{bmatrix} \Theta_{1111} & \Theta_{1121} & \Theta_{1131} & \Theta_{1112} & \Theta_{1122} & \Theta_{1132} & \Theta_{1113} & \Theta_{1123} & \Theta_{1133} \\ \Theta_{2211} & \Theta_{2221} & \Theta_{2231} & \Theta_{2212} & \Theta_{2222} & \Theta_{2232} & \Theta_{2213} & \Theta_{2223} & \Theta_{2233} \\ \Theta_{3311} & \Theta_{3321} & \Theta_{3331} & \Theta_{3312} & \Theta_{3322} & \Theta_{3332} & \Theta_{3313} & \Theta_{3323} & \Theta_{3333} \\ 2\Theta_{1211} & 2\Theta_{1221} & 2\Theta_{1231} & 2\Theta_{1212} & 2\Theta_{1222} & 2\Theta_{1232} & 2\Theta_{1213} & 2\Theta_{1223} & 2\Theta_{1233} \\ 2\Theta_{2311} & 2\Theta_{2321} & 2\Theta_{2331} & 2\Theta_{2312} & 2\Theta_{2322} & 2\Theta_{2332} & 2\Theta_{2313} & 2\Theta_{2323} & 2\Theta_{2333} \\ 2\Theta_{3111} & 2\Theta_{3121} & 2\Theta_{3131} & 2\Theta_{3112} & 2\Theta_{3122} & 2\Theta_{3132} & 2\Theta_{3113} & 2\Theta_{3123} & 2\Theta_{3133} \end{bmatrix} \tag{A2}$$

The same transformation applies to $\boldsymbol{\theta}$ in Equation (49).

DOI: 10.1002/nme

The tensor $\boldsymbol{\Lambda}$ relating non-symmetric tensors $\Delta\mathbf{F}$ and $\Delta\mathbf{f}$ in Equation (35) maps into the matrix

$$\bar{\boldsymbol{\Lambda}}=\begin{bmatrix}
\Lambda_{1111} & \Lambda_{1121} & \Lambda_{1131} & \Lambda_{1112} & \Lambda_{1122} & \Lambda_{1132} & \Lambda_{1113} & \Lambda_{1123} & \Lambda_{1133} \\
\Lambda_{2111} & \Lambda_{2121} & \Lambda_{2131} & \Lambda_{2112} & \Lambda_{2122} & \Lambda_{2132} & \Lambda_{2113} & \Lambda_{2123} & \Lambda_{2133} \\
\Lambda_{3111} & \Lambda_{3121} & \Lambda_{3131} & \Lambda_{3112} & \Lambda_{3122} & \Lambda_{3132} & \Lambda_{3113} & \Lambda_{3123} & \Lambda_{3133} \\
\Lambda_{1211} & \Lambda_{1221} & \Lambda_{1231} & \Lambda_{1212} & \Lambda_{1222} & \Lambda_{1232} & \Lambda_{1213} & \Lambda_{1223} & \Lambda_{1233} \\
\Lambda_{2211} & \Lambda_{2221} & \Lambda_{2231} & \Lambda_{2212} & \Lambda_{2222} & \Lambda_{2232} & \Lambda_{2213} & \Lambda_{2223} & \Lambda_{2233} \\
\Lambda_{3211} & \Lambda_{3221} & \Lambda_{3231} & \Lambda_{3212} & \Lambda_{3222} & \Lambda_{3232} & \Lambda_{3213} & \Lambda_{3223} & \Lambda_{3233} \\
\Lambda_{1311} & \Lambda_{1321} & \Lambda_{1331} & \Lambda_{1312} & \Lambda_{1322} & \Lambda_{1332} & \Lambda_{1313} & \Lambda_{1323} & \Lambda_{1333} \\
\Lambda_{2311} & \Lambda_{2321} & \Lambda_{2331} & \Lambda_{2312} & \Lambda_{2322} & \Lambda_{2332} & \Lambda_{2313} & \Lambda_{2323} & \Lambda_{2333} \\
\Lambda_{3311} & \Lambda_{3321} & \Lambda_{3331} & \Lambda_{3312} & \Lambda_{3322} & \Lambda_{3332} & \Lambda_{3313} & \Lambda_{3323} & \Lambda_{3333}
\end{bmatrix} \tag{A3}$$

Finally, $\bar{\mathbf{N}}_{,x}$ is the matrix reordering the derivatives of the shape functions in the following way:

$$\bar{\mathbf{N}}_{,x}=\begin{bmatrix}
\dfrac{\partial N_1}{\partial x} & 0 & 0 & \dfrac{\partial N_2}{\partial x} & 0 & 0 & \cdots \\
0 & \dfrac{\partial N_1}{\partial x} & 0 & 0 & \dfrac{\partial N_2}{\partial x} & 0 & \cdots \\
0 & 0 & \dfrac{\partial N_1}{\partial x} & 0 & 0 & \dfrac{\partial N_2}{\partial x} & \cdots \\
\dfrac{\partial N_1}{\partial y} & 0 & 0 & \dfrac{\partial N_2}{\partial y} & 0 & 0 & \cdots \\
0 & \dfrac{\partial N_1}{\partial y} & 0 & 0 & \dfrac{\partial N_2}{\partial y} & 0 & \cdots \\
0 & 0 & \dfrac{\partial N_1}{\partial y} & 0 & 0 & \dfrac{\partial N_2}{\partial y} & \cdots \\
\dfrac{\partial N_1}{\partial z} & 0 & 0 & \dfrac{\partial N_2}{\partial z} & 0 & 0 & \cdots \\
0 & \dfrac{\partial N_1}{\partial z} & 0 & 0 & \dfrac{\partial N_2}{\partial z} & 0 & \cdots \\
0 & 0 & \dfrac{\partial N_1}{\partial z} & 0 & 0 & \dfrac{\partial N_2}{\partial z} & \cdots
\end{bmatrix} \tag{A4}$$

ACKNOWLEDGEMENTS

The financial support from European Community (contract number AST4-CT-2005-516183) and from Consejo Nacional de Investigaciones Científicas y Técnicas (grant PIP 5271) is gratefully acknowledged.

DOI: 10.1002/nme

REFERENCES

1. Beck JV, Woodbury KA. Inverse problems and parameter estimation: integration of measurements and analysis. *Measurement Science and Technology* 1998; **9**:839–847.
2. Govindjee S, Mihalic PA. Computational methods for inverse finite elastostatics. *Computer Methods in Applied Mechanics and Engineering* 1996; **136**:47–57.
3. Govindjee S, Mihalic PA. Computational methods for inverse deformations in quasi-incompressible finite elasticity. *International Journal for Numerical Methods in Engineering* 1998; **43**:821–838.
4. Yamada T. Finite element procedure of initial shape determination for hyperelasticity. *Structural Engineering and Mechanics* 1997; **6**(2):173–183.
5. Samtech SA. *Samcef/Mecano v11 User Manual*. Samtech S.A., 2005.
6. Ogden RW. *Non-linear Elastic Deformations*. Dover: New York, 1997.
7. Zienkiewicz OC, Taylor RL. *The Finite Element Method*, vol. 2 (5th edn). Solid and Structural Mechanics. Butterworth-Heinemann: London, 2000.
8. Truesdell C, Noll W. The non-linear field theories of mechanics. In *Encyclopedia of Physics*, Flügge S (ed.), vol. 3. Springer: Berlin, 1965.
9. Thoutireddy P. Variational arbitrary Lagrangian–Eulerian method. *Ph.D. Thesis*, California Institute of Technology, 2003.
10. Thoutireddy P, Ortiz M. A variational r-adaption and shape-optimization method for finite-deformation elasticity. *International Journal for Numerical Methods in Engineering* 2004; **61**:1–21.

DOI: 10.1002/nme